Nonequilibrium energy gaps in carbon nanotubes: Role of phonon symmetries

Luis E. F. Foa Torres,[1,2,*] Rémi Avriller,[2] and Stephan Roche[2]
[1]*CEA Léti-MINATEC, CEA-LETI, 17 avenue des Martyrs, 38054 Grenoble, France*
[2]*CEA, Institut des Nanosciences et Cryogénie, 17 avenue des Martyrs, 38054 Grenoble, France*
(Received 9 October 2007; revised manuscript received 30 April 2008; published 8 July 2008)

We report on a theoretical study of inelastic backscattering processes and quantum transport in metallic carbon nanotubes. The consequences of a Peierls-like mechanism due to *e*-ph interaction with optic phonons in the transport properties is explored. The occurrence of nonequilibrium energy gaps driven by an applied bias voltage is derived from a nonperturbative treatment of electron-phonon coupling with longitudinal optic as well as $K\,A_1'$ modes. The case of armchair tubes is explicitly considered, and further generalizations to tubes of arbitrary helicity are outlined.

DOI: 10.1103/PhysRevB.78.035412 PACS number(s): 73.63.Fg, 72.10.Di, 73.23.−b, 05.60.Gg

I. INTRODUCTION

Since the early days of the development of the quantum theory of solids,[1] the role played by the coupling between lattice vibrations and electrons has been a great issue of concern. Among a large variety of physical phenomena, the electron-phonon (el-ph) interaction was in particular shown to be at the origin of BCS superconductivity,[2,3] or to be responsible for the metal-insulator (Peierls) transition in organic materials and novel phonon-mediated charge transport mechanisms (known as polaronic effects) in conducting polymers.[4–6]

More recently, thanks to the advent of miniaturization techniques, the effects of *e*-ph interaction on electronic transport could be challenged in low dimensional systems such as semiconductor heterostructures, quantum dots, as well as the ultimate limit of single molecules contacted to electrodes.[7–9] Electron-phonon interactions in these systems are crucial to understand decoherence[10,11] and produce captivating phenomena such as phonon-assisted tunneling.[12]

Carbon based materials such as polymers, graphitic structures, and fullerenes have also captured much recent attention. Among such family, hollow cylinders with nanometer scale diameter formed by rolling a graphene sheet,[13] today known as single-walled carbon nanotubes (nanotubes hereafter), stand as one of the major driving forces of fundamental research due to their outstanding mechanical and electrical properties.[14–16] At the same time, these properties have attracted much technological interest and foreseen applications include nanotube-based field effect transistors,[17] interconnects[18] and light detectors.

In this work, we will focus on the effects of *e*-ph interaction on transport through carbon nanotubes (CNTs). By using a many-body approach beyond mean-field theory, the occurrence of nonequilibrium energy gaps will be demonstrated in metallic CNTs (chiral and achiral) driven by longitudinal optic and $K\,A_1'$ phonons, the same modes that lead to Peierls instability and Kohn anomalies.

A. Effects of electron-phonon interaction on electron and phonon bandstructures: Peierls Instability and Kohn Anomaly.

Some of the most interesting manifestations of *e*-ph interactions lie beyond the realm of the usual Fermi golden rule,[19] where the approximation of separability between electron and phonon degrees of freedom fails. A remarkable example is the Peierls instability: Long time before the synthesis of quasi-one-dimensional materials was first achieved, Peierls[20] predicted that quasi-one-dimensional metals would be unstable against a distortion of the network modulating the interatomic distances with period $2\pi/2k_F$, where k_F is the Fermi wave number. The interaction between electrons and phonons with a specially tuned wave vector can drive this Peierls instability, leading to a structural change and the opening of a gap at the Fermi surface. As pointed out by Fröhlich,[21] this occurs below a certain critical temperature T_c (when the phonon frequency is sufficiently small or the *e*-ph coupling constant is strong enough[22]). It is interesting to note that historically the instability as originally proposed by Peierls[20] is almost independent of the underlying mechanism. The missing ingredient was introduced by Fröhlich who proposed that the Peierls transition results from a phonon condensation in wave-vector space,[21] thereby giving a central role to the *e*-ph the interaction.

For undoped polymers such as polyacetylene, the Peierls-Fröhlich mechanism was demonstrated to be crucial to understand their intrinsic semiconducting nature at room temperature, with energy gaps in order of 1–2 eV.

Later, after the discovery of CNTs, the existence of a true one-dimensional (1D) metallic state came out as a great surprise.[14,16] Indeed, in contrast to other π-conjugated materials, the Peierls instability is not operative in CNTs,[16] except at low temperatures (~ 10 K),[23] or for very short tube radius (~ 0.2 nm).[24]

Notwithstanding, electron-phonon coupling triggers significant corrections of the vibrational band structure, known as Kohn Anomalies (KA),[25] that persist even at ambient conditions, well above the critical temperature.[26,27] KA appear as a softening of a specific phonon modes (longitudinal-optic phonons (ΓE_{2g}) and $K\,A_1'$ phonons), close to which the dispersion relation becomes nonanalytic.[28] However, differently to the Peierls transition, the phonon energy remains finite (nonzero frequency) and phonons experience a *dynamic* softening. The widely used adiabatic approximation (zero frequency) were recently shown to fail to reproduce experimental data for the case of graphene.[29] Further theoretical[30,31] as well as experimental[32] works on nanotubes have also been

recently reported. In Refs. 26 and 27, the phonon softening for the longitudinal-optic mode was linked to the Peierls mechanism.

B. Effects of electron-phonon interaction on transport

Nanotubes present an anomalously low sensitivity to disorder-induced backscattering[33] and unique spectral features.[34] Transport experiments on metallic tubes with low resistance contacts evidence ballistic transport in the low bias regime.[35] This is in sharp contrast with the behavior observed at high bias where the resistance increase leads to a current saturation attributed to inelastic backscattering by optic phonons.[36–38]

These experiments have triggered several theoretical studies using the Boltzmann transport equation, and treating perturbatively the *e*-ph coupling within the Fermi golden rule approximation.[39–41] Assuming an equilibrium phonon population, the initial theoretical estimate of the inelastic mean-free path was, however, shown to be in quantitative disagreement with experimental values (see Ref. 42 and references therein). Later, such discrepancy was tentatively explained assuming an enhanced phonon population (hot phonon generation), resulting from nonequilibrium electron transport.[43] Further, Boltzmann transport equations coupling electron and phonon dynamics were self-consistently solved, yielding good fitting of experimental current-voltage characteristics,[44,45] but with a strong enhancement of the optic phonon occupation number in the steady state. The obtained values $n=1/(e^{\hbar\omega/k_bT_{\mathrm{eff}}}-1)$ were found to be $\sim 3-20$, corresponding to effective temperatures T_{eff} of several thousands of Kelvins.

Recent Raman spectroscopy experiments on metallic nanotubes showed an increase in the G mode phonon temperature under biased conditions, in contrast with radial breathing modes which remain close to thermal equilibrium.[46] Notwithstanding, the optic effective phonon temperature was found to reach only 500 K for bias voltage as large as 3 V, at least one order of magnitude lower than the predicted one.[44]

Transport calculations beyond the semiclassical Boltzmann equation and including some electron-phonon effects have been reported in Refs. 47 and 48. In, Ref. 47, the conductance of a metallic nanotube computed with the Landauer formula was averaged over many different atomic configurations derived from molecular dynamics of nanotube devices at room temperature. Differently, in Ref. 48, the propagation of a quantum wave packet was investigated incorporating time dependent changes of the electronic couplings between nearest-neighbor orbitals, followed by a Kubo conductance calculation. Other studies have followed a similar approach,[49] but such frameworks assume adiabadicity of the electron-phonon system which turn out to be a too severe limit, as discussed hereafter.

In this context, a key question is whether any quantum phenomenon beyond the Fermi golden rule could manifest in nonequilibrium situation, and what could be its experimental signature. This is particularly relevant in CNTs since a strong enhancement of *e*-ph coupling could be driven by the low dimensionality of the system.

C. This work

In low dimensional systems, the KA and the Peierls-Fröhlich mechanism are not independent phenomena.[22,26,27,50,51] For carbon nanotubes, this was already emphasized by Dubay and co-workers[26,27] and Samsonidze *et al.*[51] Indeed, KAs can be regarded as a precursor of the Peierls transition[50] which occurs once the selected phonon mode softens enough to fall within the available phase space for scattering. A natural question is whether this could have any consequence on transport at intermediate temperatures ($T>T_c$) once a high enough bias voltage is supplied.

A related mechanism was recently proposed in Refs. 52 and 53 for longitudinal-optic phonons in zigzag tubes. It was shown that if a single mode dominates, *nonequilibrium energy gaps* (NEEG) open at half the phonon energy above the charge neutrality point (CNP) which, in turn, is manifested as a plateau in the *I-V* characteristics for bias voltages in the order of the phonon energy.

In the present study, these NEEG are shown to be intrinsically related with electron-phonon coupling through phonon symmetries, and are observed for *both* types of high-symmetry optic phonons leading to Peierls instabilities, namely: longitudinal optic (ΓE_{2g}) and $K\ A_1'$ phonons. Additionally, we provide a generalization of our prior study for achiral (armchair) and chiral metallic tubes of any helicity. Given that these modes do not compete, their associated NEEG result in superimposed plateaus in the current-voltage characteristics at moderate temperatures. Besides, since KAs are found for the same phonon symmetries, we suggest that a joint measurement of current-voltage characteristics and Raman spectrum should be able to unveil the occurrence of these many-body effects.

The paper is organized as follows. In Sec. II, the total Hamiltonian is introduced. Section III presents the main analytical results and interpretation of NEEG, together with numerical calculations for transmission probabilities and voltage dependent current densities. Conclusions and open questions are collected in Sec. IV.

II. HAMILTONIAN MODEL

We start by defining our effective Hamiltonian that describes electron and phonon degrees of freedom together with the *e*-ph interaction. For simplicity, an infinite CNT is considered and the electrons are allowed to interact with phonons only in a finite section of length L of the CNT. The contribution from two phonon branches will be considered separately: $\Gamma\ E_{2g}$ and $K\ A_1'$ phonons. The Hamiltonian is written as a sum of an electronic term, a phonon contribution and an *e*-ph interaction term:

$$H = H_e + H_{\mathrm{ph}} + H_{e\text{-ph}}. \tag{1}$$

The electronic part is described through a π-orbitals effective model (i.e., a single π orbital per carbon atom):

$$H_e = \sum_i E_i c_i^+ c_i - \gamma_0 \sum_{\langle i,j\rangle} (c_i^+ c_j + \mathrm{H.c.}), \tag{2}$$

where c_i^+ and c_i are the creation and annihilation operators for electrons at site i, γ_0 is the π-π integral overlap, the

second summation is restricted to nearest neighbors in the CNT. E_i is set to zero $\forall i$ in case of clean CNTs (no superimposed elastic disorder).

For a given phonon branch, the corresponding Hamiltonian is given by: $H_{\mathrm{ph}}=\Sigma_q \hbar\omega_q b_q^+ b_q$, where b_q^+ and b_q are the phonon operators for phonons with wave vector q.

The last contribution to Eq. (1) describes the e-ph interaction term. Lattice vibrations will produce a modulation of the bond's length, thereby changing the hopping matrix elements. To account for these phenomena, the Su-Schrieffer-Heeger Hamiltonian is employed.[54] In this model, the contribution arising from the phonons is derived by modulating the electronic coupling terms keeping only the linear corrections to the atomic displacements from equilibrium. This reads: $\gamma_{i,j}=\gamma_0+\alpha\hat{\delta}_{i,j}\cdot\delta\vec{Q}_{i,j}$, where $\hat{\delta}_{i,j}$ is a unit vector in the bond direction, whereas $\delta\vec{Q}_{i,j}$ sets the relative displacement between neighboring carbon atoms, and α is the e-ph coupling strength defined as the derivative of γ_0 with respect to the bond-length displacement ($\alpha=\alpha_0\simeq 7$ eV/Å is estimated from Ref. 55). Further quantization of the atomic displacements gives the many-body e-ph interaction term:

$$H_{e\text{-ph}}=\sum_{q,\langle i,j\rangle_{\mathrm{vib}}}[\gamma_{i,j}^{e\text{-ph}(q)}c_i^+c_j(b_q+b_{-q}^+)+\mathrm{h.c.}]. \qquad (3)$$

The symmetry of the phonon mode is encoded through the polarization vectors $\vec{e}_i$ that enter into the e-ph matrix elements $\gamma_{i,j}^{e\text{-ph}(q)}$, and which turn out to be proportional to the projection of the lattice displacements along the bond direction $\hat{\delta}_{i,j}$ $[\hat{\delta}_{i,j}\cdot(\vec{e}_i-\vec{e}_j)]$.

At this point, instead of considering all the phonon modes in the branch on the same footing, we will consider exactly the interaction between electrons and a single phonon mode with wave vector q_0; in our Hamiltonian model, we take $\gamma_{i,j}^{e\text{-ph}(q)}=\alpha\sqrt{\hbar/(m\omega_0)}\hat{\delta}_{i,j}\cdot(\vec{e}_i-\vec{e}_j)\times\delta_{q,q_0}$, where $q_0=0$ for the case of longitudinal-optic phonons and $q_0=K$ for the branch corresponding to K A_1' phonons.[56] A precise calculation of the Hamiltonian parameters would involve a self-consistent treatment in a nonequilibrium situation which is beyond the scope of this paper. The above effective one-mode Hamiltonian[52] is in the spirit of the Peierls-Fröhlich mechanism,[21,22,57] the main point being that a mode with an especially tuned wave vector is dominant while the others can be considered within perturbation theory.

To investigate transport properties with such Hamiltonian, a Fock-space approach will be used following Refs. 52 and 58–60. The key point of the approach is to express the many-body Hamiltonian (one electron plus phonons) in Fock-space basis. This leads to an effective single-particle problem in an enlarged space, thereby allowing the calculation of the transmission probabilities between the different elastic and inelastic channels. In contrast to semiclassical transport approaches based on the Fermi golden rule, the method is nonperturbative in the e-ph interaction strength. Besides, the energy exchange due to e-ph processes is fully taken into account. In other words, the obtained solution is beyond the Fermi golden rule and the adiabatic approximation. The Pauli principle is included in the finite bias calculation of the current by a proper state occupancy counting statistics.[60]

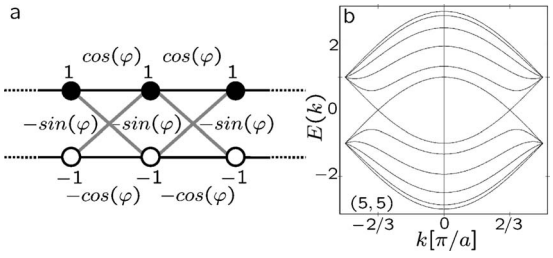

FIG. 1. (a) Scheme for the Hamiltonian corresponding to each of the decoupled circumferential modes obtained after the change of basis transformation. (b) Bandstructure for a (5,5) tube obtained by using the decomposition shown in (a). Energies are in units of γ_0.

The problem can be first simplified by an appropriate change of basis for the electronic degrees of freedom (mode decomposition). Although in the following sections we deal with armchair tubes, generalizations to arbitrary helicity are straightforward and will be outlined at the end of Sec. III.

A. Mode decomposition for the electronic degrees of freedom

For (N,N) armchair tubes, carbon atoms are arranged into layers lying on planes perpendicular to the tube axis. By applying a change of basis transformation within each layer subspace, it is possible to obtain a set of decoupled circumferential modes.[61] The Hamiltonian for each of these modes is represented in Fig. 1, where the parameter $\varphi=\pi j/N$ with $j=0,1,\ldots N-1$. Note that the circumferential mode contributing to the density of states at the charge neutrality point (massless subbands) corresponds to $\varphi=0$, which in turn leads to two independent chains, called channels from hereon. This greatly simplifies our subsequent analysis of the effects of e-ph interaction close to the CNP.

III. ELECTRON-PHONON INTERACTION EFFECTS AND PEIERLS-FRÖHLICH MECHANISM

In this section, we consider the effects of optic phonons. One will focus on the phonons of highest symmetry which couple electronic states close to the Fermi surface, namely the longitudinal optic and zone-boundary K A_1' vibrational modes. The main idea of the computational scheme is to write the Hamiltonian in a many-body basis for a single electron interacting with phonons. This allows the calculation of elastic and inelastic transmission probabilities[58,59] which are then used as inputs in the self-consistent calculation of the current at finite bias voltage.[60]

A. Longitudinal optic phonons

1. Many Body Hamiltonian in Matrix Form

In the case of armchair tubes, Γ E_{2g} phonons produce an out-of-phase displacement of neighboring atoms along the axis direction. This is represented in Fig. 2. In the following, the effects of this mode are first analyzed based on symmetry considerations. We start by writing the many-body Hamiltonian in matrix form. The selected basis includes both the

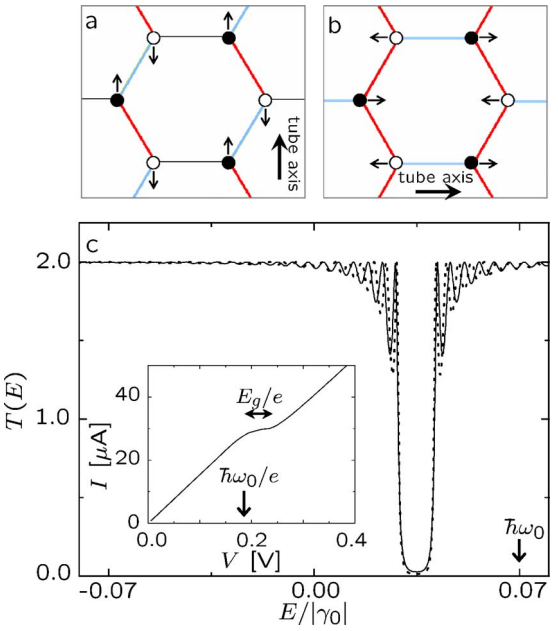

FIG. 2. (Color online) Representation of the atomic displacements for longitudinal optical modes in armchair (a) and zigzag tubes (b). (c) Total transmission probability as a function of the incident electron energy in the presence of e-ph interaction with longitudinal optical modes shown in (a) and (b). The full line corresponds to a (10,10) tube whereas the dotted line is for a (24,0) tube. Phonon population is assumed to be in equilibrium ($n_0=0$). The phonon energy is taken to be $\hbar\omega_0=0.07\gamma_0$.

electronic and the phonon degrees of freedom: $\{|k^{(s)},n\rangle \equiv |k^{(s)}\rangle \otimes |n\rangle\}$ where $|k^{(s)}\rangle$ is a state with wave vector k in the subband indicated with the index s; $|n\rangle$ is a state with n phonons in the tube. In Fig. 2(a), the carbon-carbon bonds are represented by lines with different tones (colored online) according to the relative phase of the respective atomic displacements in real space. It is seen that within each layer there are no changes in the bond lengths up to first order in the atomic displacements, while the bond lengths between atoms of neighboring layers include two such tones or "colors" (which correspond to out-of-phase motion). As a consequence, the e-ph interaction with this phonon mode does mix different subbands.

A scheme with the dispersion relation $(\varepsilon^{(0)}(k,n) = \langle k,n|H_e+H_{\text{ph}}|k,n\rangle)$ of the e-ph Fock states for the subbands at the CNP is shown in Fig. 3(a). At the points marked with rounded symbols, different curves intersect and, interestingly, $H_{e\text{-ph}}$ introduces a nonvanishing matrix element between these states. The degeneracy is thus lifted, giving rise to the opening of energy gaps at $\hbar\omega_0/2$ above (below) the CNP due to phonon emission (absorption). This effect was previously unveiled in Ref. 52, analytically and numerically for longitudinal-optic phonons in zigzag tubes [see Fig. 2(b)], whereas only numerical results were available for armchair tubes, without any explicit analysis of the involved Fock states. Although the crossing points involving higher order phonon processes lead to minigaps (second order in the e-ph interaction strength) for the case of semiconducting tubes,[53] they do not lead to any feature in the case of metallic tubes where $H_{e\text{-ph}}$ has a vanishing matrix element between these states.

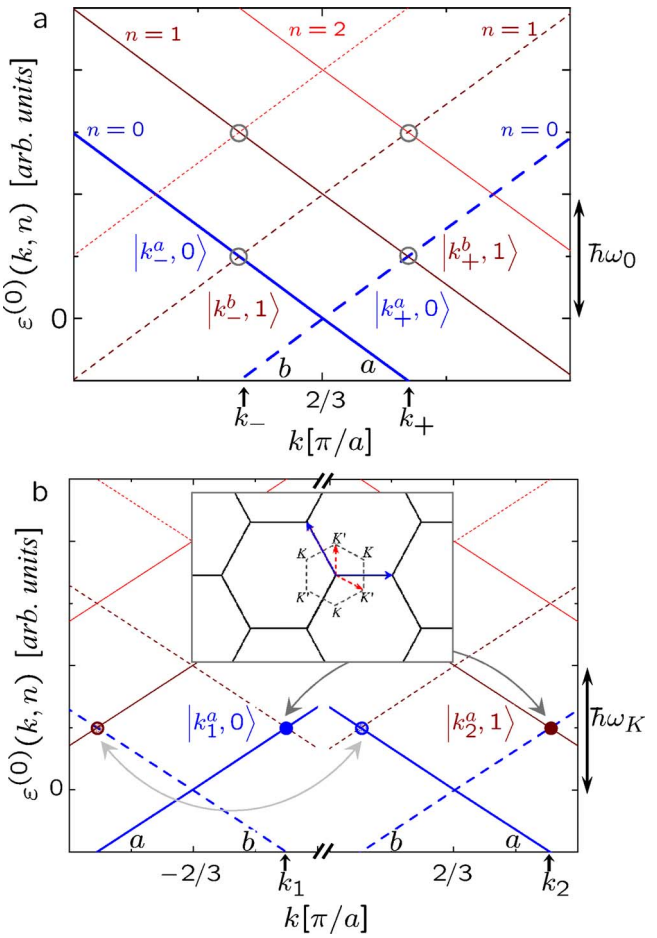

FIG. 3. (Color online) Dispersion relations for uncoupled electrons and phonons in armchair tubes. E-ph processes leading to the main features close to the CNP are represented for (a) LO phonons and (b) K A_1' phonons. The inset in (b) shows the reciprocal lattice of graphene and its reciprocal-lattice vectors (full blue lines), the reciprocal-lattice vectors of the colored lattice (dashed red lines) are shown as well.

2. Results

Figure 2(c) shows the total transmission probability from the left (L) to the right (R) electrodes $T(E) = \Sigma_n T_{(L,n_0)\to(R,n)}(E)$ for a (10,10) tube as a function of the incident's electron energy $E(n_0=0)$. Results for the same longitudinal-optic mode in a zigzag (24,0) tube are also shown with a dotted line. The main features are again the appearance of dips of different widths at $E\sim\hbar\omega_0/2$ above the CNP ($E=0$) that develop into full gaps as L increases. The transmission suppressions at $E\sim\hbar\omega_0/2$ are complemented by an increase in the probability of *inelastic backscattering with the emission of a phonon*. These processes are represented in Fig. 3(a).

The small difference between both curves in Fig. 2(c) is due to the different geometry related factors (that result from projecting the atomic displacements along the bond directions). This can quantified by using the mode decomposition introduced before, it can be shown that the gap amplitude for zigzag tubes contains a geometrical prefactor $1+\cos(\pi/3)$ whereas the one for armchair tubes is $2\cos(\pi/6)$. Another

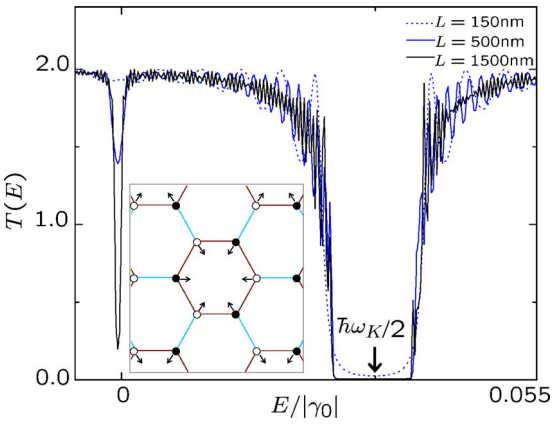

FIG. 4. (Color online) Total transmission probability as a function of the incident electron energy in the presence of e-ph interaction with $K\,A_1'$ phonons shown in (a) and (b). Different curves are for different values of L. The results correspond to a (10,10) tube and the phonon population is assumed to be in equilibrium ($n_0=0$). The phonon energy is taken to be $\hbar\omega_K=0.055\gamma_0$. Inset: Representation of the atomic displacements for $K\,A_1'$ phonons.

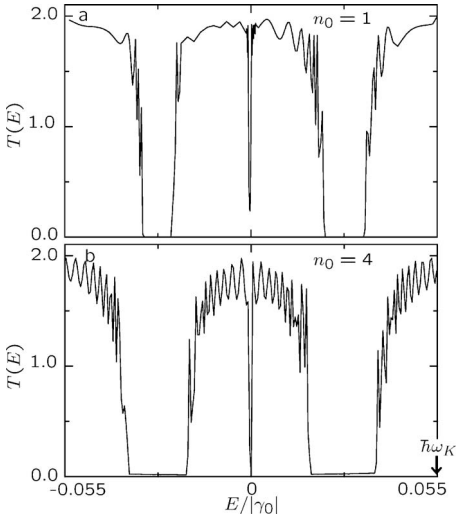

FIG. 5. Same as Fig. 4 for $n_0=1$ and $n_0=4$. Additional NEEGs open at energy $E\sim-(\hbar\omega_K/2)$ corresponding to an increase in the probability of inelastic backscattering with the absorption of a phonon. The width of NEEG is also shown to increase with phonon number in the system according to the rescaled e-ph matrix elements with a factor $\sqrt{n_0+1}(\sqrt{n_0})$ for phonon emission (absorption) processes.

point to notice is the scaling of the transmission minimum at $E\sim\hbar\omega_0/2$ with the tube length, as shown in Ref. 52, $T(E\sim\hbar\omega_0/2)$ scales as $\exp(-L/\xi)$, with a decay length ξ that is inversely proportional to the energy gap.

What about the observable consequences of this phenomenon? Since at low bias voltages these inelastic processes are forbidden by Pauli blocking, the effect presented before will not lead to a true gap in a thermodynamic equilibrium state. Instead, it will be manifested, once the bias voltage is high enough to overcome Pauli blocking, as a plateau in the current-voltage characteristics for bias voltages in the order of the phonon energy,[52] see inset of Fig. 2(c). Our estimation for this gap gives $E_g\sim 32$ meV, therefore it should be observable at moderate temperatures.

B. $K\,A_1'$ phonons

1. Many-body Hamiltonian in matrix form

The distortion produced by $K\,A_1'$ phonons is represented in Fig. 4 inset. The drawing style of C–C bonds (color online) is made according to the relative phase of the atomic displacements. Interestingly, it can be shown that the e-ph interaction does not mix the two electronic channels close to the CNP. Another important observation is that the period of the colored lattice (which is the period introduced by the e-ph interaction Hamiltonian) is $3a(a\equiv\sqrt{3}a_{cc}/2)$. Therefore, e-ph coupling has nonvanishing matrix element connecting states of reciprocal space differing by $K=4\pi/(3a)$.

2. Results

The total transmission probability $T(E)$ for a (10,10) tube in the presence of e-ph interaction with this mode is shown in Fig. 4 as a function of the incident's electron energy E. Different curves correspond to different values of L. The curves corresponding to initial phonon occupations $n_0=1$ and $n_0=4$ for a tube with $L=1.5$ μm are shown in Fig. 5 (top and bottom panels respectively). Two main features are observed: a) the appearance of dips of different widths at $E\sim\hbar\omega_K/2$ above the CNP ($E=0$) as for the case of LO phonons; and b) a minigap at the CNP. Both of them develop into full gaps as L increases. While the transmission suppressions at $E\sim\hbar\omega_K/2$ are complemented by an increase in the probability of *inelastic backscattering with the emission of a phonon*, the one at the CNP corresponds to a *phonon-mediated increase in the elastic reflectance*.

Closer inspection of the possible e-ph processes show that the gap at $E\sim\hbar\omega_K/2$ in the one-particle excitation spectrum is due to the mixing of the states at different K points in the Brillouin zone [see scheme in Fig. 3(b)]. The degeneracy between the corresponding Fock states is lifted by $H_{e\text{-ph}}$ leading to a strong inelastic backscattering at $E\sim\hbar\omega_K/2$ above (below) the CNP due to phonon emission (absorption). Note that for both LO and $K\,A_1'$ phonons, the gap is slightly shifted from $E\sim\hbar\omega_K/2$ due to higher order contributions involving other nondegenerate intermediate states, a fact that is noticeable in Fig. 4 because of the energy scale chosen.

The minigap at the CNP has a more subtle origin. Its physical origin is the lifting of degeneracies between the states close to the CNP produced by a virtual process involving phonon emission and reabsorption. Specifically, the states $|K,n_K=0\rangle$ and $|K',n_K=0\rangle$ at the CNP, where K and K' label the electronic states at those points and n_K is the occupation of the $K\,A_1'$ phonon mode, are connected via a second-order virtual process (emission and reabsorption of a phonon) through the intermediate state $|K',n_K=1\rangle$. Since the intermediate state is a virtual one, differing in energy by $\hbar\omega_K$ from the initial and final ones, the resulting gap is second order in the e-ph interaction strength and inversely proportional to the phonon energy. The reason why this minigap does not appear for LO phonons is rooted in the symmetry of

the phonon mode which establishes selection rules giving a vanishing matrix element with the possible intermediate (virtual) states.

These nonequilibrium energy gaps will manifest, in the same way as for longitudinal-optic phonons, namely a plateau in the current-voltage curve for bias voltages in the order of $\hbar\omega_K$. Since the phonon energies $\hbar\omega_\Gamma$ and $\hbar\omega_K$ differ by more than the estimated gap ($\hbar\omega_\Gamma - \hbar\omega_K \sim 40$ meV), these processes are not expected to compete. As evidenced in Fig. 5, the eventual increase in the phonon occupation number in the nanotube may have a strong effect on the resulting inelastic backscattering probability, and thus on the computed NEEG widths. This suggests that a weak thermalization rate, as produced in experiments using suspended CNTs, will favor an enhancement of these nonequilibrium effects. Further work is clearly needed to achieve quantitative predictions. This challenging issue is beyond the scope of the present work and would involve a self-consistent calculation of *e*-ph couplings together with a solution of the electrostatics and the phonon dynamics.

Regarding the minigap, one must emphasize that the virtual process leading to it requires for the intermediate state to be empty. Pauli blocking will therefore suppress it at low bias voltages and the *I*-*V* characteristics will be affected at bias voltages in the order of $\hbar\omega_K$ (this contribution will be additive to the one due to the gap at $E \sim \hbar\omega_K/2$).

C. Further generalizations

The performed analysis for the K point phonons in armchair tubes can be extended to incorporate the effect of the same mode on tubes of arbitrary helicity. Although a direct calculation is beyond the scope of this manuscript, we present here an argument showing that the matrix element of the *e*-ph Hamiltonian between the degenerate Fock states is nonvanishing for arbitrary helicity tubes. This leads to the opening of nonequilibrium gaps as shown for armchair and zigzag tubes.

The main remark is that the K point phonons considered here couple the electronic states around K with those around K' independently of the tube helicity, therefore leading to the same effect as predicted before. This can be shown by scrutinizing the periodicity of the *e*-ph interaction whose information is encoded in the colored lattice (Fig. 4 inset). This can be seen in Fig. 3(b) inset, where both the primitive vectors of the reciprocal lattice of graphene (full blue) and that of the colored lattice (dashed red lines) are depicted. For a given axis direction, after zone folding, one can see that k and k' (with k chosen around K and k' chosen around K' such that $|k-k'|=2\pi/(\sqrt{3}|\vec{C}|)(n1+n2)$, $\vec{C}=n_1\vec{a}_1+n_2\vec{a}_2$ being the chiral vector) are connected by the primitive vectors of the colored lattice (i.e., the *e*-ph interaction). Then, the reasoning for the corresponding Fock states proceeds as before but with the new matrix element that depends on a geometrical factor related to the tube helicity and the symmetry of the phonon mode.

A similar argument follows for the longitudinal modes studied in the Sec. II. However, in this case, it must be noted that the graphene mode that produces longitudinal axial distortion (for armchair tubes) [Fig. 2(a)] is transversal for zigzag tubes and does not produce any feature. The mode shown in Fig. 2(b) is responsible for the same phenomenon.

IV. CONCLUSIONS

Motivated by the physics of the Peierls-Fröhlich mechanism,[20,21] which leads to the Peierls transition at low enough temperatures ($T<T_c$) in quasi-one-dimensional systems, we have explored its possible consequences in a nonequilibrium transport situation at high bias and temperatures above T_c. The main result of our model is the opening of nonequilibrium energy gaps at half the phonon energy above (below) CNP, due to the interaction of electrons with a single phonon mode as in the Peierls-Fröhlich mechanism which produces inelastic backscattering with phonon emission (absorption). However, in contrast with the Peierls transition, there is here no static distortion of the lattice, since phonons retain their intrinsic dynamics, although their energy is slightly softened.

The experimental observation of NEEG in clean metallic nanotubes should be possible through the onset of a current plateau (of width in order of $\sim$30 meV) for bias voltages ($\sim$150–190 mV) at low enough temperatures, although heating of the phonon system might enhance these features.

The main achievements of this paper are: a) generalization of the analysis in Ref. 52 for longitudinal-optic phonons in zigzag tubes to armchair tubes. This analysis, which is based on the use of a mode decomposition for the electronic degrees of freedom (similar to the one used previously for zigzag tubes) allows for a quantitative interpretation of the numerical results. b) Extension of the above scenario to the case of K A_1' phonons in armchair and arbitrary helicity tubes, highlighting the key role of phonon symmetries in the reported phenomena. To such end we have analyzed in detail the case of armchair tubes and outlined generalization to tubes with arbitrary helicity.

Recently, the effect of phonon symmetries on the electronic spectra was also discussed in Ref. 51. Although the occurrence of energy gaps was outlined, the nonequilibrium situation in which these NEEG truly develop is beyond the scope of the adiabatic approximation used in Ref. 51. Indeed, in this treatment, the failure to properly account for the energy exchange in the *e*-ph processes would lead to a real gap at low energy. In contrast, our approach that goes beyond the adiabatic limit naturally introduces the Pauli blocking mechanism which brings a bias threshold below which phonons do not play any role.

Although crude, our model captures the main ingredient behind the Peierls-Fröhlich mechanism and the experimental observation of its consequences in the nonequilibrium response of carbon nanotubes or related materials could open an exciting path toward a promising *terra incognita*. For instance, a joint Raman and transport experiment in high bias conditions on a single CNT, could allow to simultaneously reveal the activation of optic phonon modes and their effect on current-voltage characteristics.

ACKNOWLEDGMENTS

LEFFT acknowledges F. Mauri for useful comments and the support of the Alexander von Humboldt Foundation. This work was supported by the ChimTronique program, the ANR/PNANO "ACCENT" project funded by the French National Research Agency (ANR), by the Carnot Institut (LETI) and by the European Union project "Carbon nanotube devices at the quantum limit" (CARDEQ) under contract No. IST-021285-2.

*Present address: Institute for Materials Science, Dresden University of Technology, D-01062 Dresden, Germany

[1] P. W. Bridgman, Phys. Rev. **17**, 161 (1921); R. E. Peierls, Ann. Phys. **4**, 121 (1930).
[2] J. Bardeen, Rev. Mod. Phys. **23**, 261 (1951).
[3] M. Tinkham, *Introduction to Superconductivity*, 2nd ed. (Dover, New York, 2004).
[4] A. J. Heeger, S. Kivelson, J. R. Schrieffer, and W. P. Su, Rev. Mod. Phys. **60**, 781 (1988).
[5] A. J. Heeger, Rev. Mod. Phys. **73**, 681 (2001).
[6] R. Peierls, *More Surprises in Theoretical Physics* (Princeton University Press, Princeton, NJ, 1991).
[7] C. Joachim, J. K. Gimzewski, and A. Aviram, Nature (London) **408**, 541 (2000).
[8] A. Pecchia and A. Di Carlo, Rep. Prog. Phys. **67**, 1497 (2004).
[9] *Introducing Molecular Electronics*, Lecture Notes in Physics Vol. 680, edited by G. Cuniberti, G. Fagas, and K. Richter (Springer, New York, 2005).
[10] H. M. Pastawski, L. E. F. Foa Torres, and E. Medina, Chem. Phys. **281**, 257 (2002).
[11] S. Chrakravarty and A. Schmid, Phys. Rep. **140**, 193 (1986).
[12] M. Galperin, M. A. Ratner, and A. Nitzan, J. Phys.: Condens. Matter **19**, 103201 (2007).
[13] S. Iijima, Nature (London) **354**, 56 (1991); S. Iijima and T. Ichihashi, *ibid.* **363**, 603 (1993).
[14] R. Saito, M. Fujita, G. Dresselhaus, and M. S. Dresselhaus, Phys. Rev. B **46**, 1804 (1992).
[15] J.-C. Charlier, X. Blase, and S. Roche, Rev. Mod. Phys. **79**, 677 (2007).
[16] J. W. Mintmire, B. I. Dunlap, and C. T. White, Phys. Rev. Lett. **68**, 631 (1992).
[17] P. L. McEuen, M. S. Fuhrer, and H. Park, IEEE Trans. Nanotechnol. **1**, 78 (2002).
[18] J. C. Coiffic, M. Fayolle, S. Maitrejean, L. E. F. Foa Torres, and H. Le Poche, Appl. Phys. Lett. **91**, 252107 (2007).
[19] For an interesting discussion on Fermi golden rule and its limits see H. M. Pastawski, Physica B **398**, 278 (2007); E. R. Fiori and H. Pastawski, Chem. Phys. Lett. **420**, 35 (2006).
[20] R. Peierls, *Quantum Theory of Solids* (Clarendon, Oxford, 1955).
[21] H. Fröhlich, Proc. R. Soc. London, Ser. A **223**, 296 (1954).
[22] J. V. Pulé, A. Verbeure, and V. Zagrebnov, J. Stat. Phys. **76**, 159 (1994).
[23] M. T. Figge, M. Mostovoy, and J. Knöester, Phys. Rev. Lett. **86**, 4572 (2001).
[24] D. Connetable, G.-M. Rignanese, J.-C. Charlier, and X. Blase, Phys. Rev. Lett. **94**, 015503 (2005).
[25] W. Kohn, Phys. Rev. Lett. **2**, 393 (1959).
[26] O. Dubay, G. Kresse, and H. Kuzmany, Phys. Rev. Lett. **88**, 235506 (2002).
[27] O. Dubay and G. Kresse, Phys. Rev. B **67**, 035401 (2003).
[28] S. Piscanec, M. Lazzeri, F. Mauri, A. C. Ferrari, and J. Robertson, Phys. Rev. Lett. **93**, 185503 (2004).
[29] S. Pisana, M. Lazzeri, C. Casiraghi, K. S. Novoselov, A. K. Geim, A. C. Ferrari, and F. Mauri, Nat. Mater. **6**, 198 (2007).
[30] N. Caudal, A. M. Saitta, M. Lazzeri, and F. Mauri, Phys. Rev. B **75**, 115423 (2007).
[31] S. Piscanec, M. Lazzeri, J. Robertson, A. C. Ferrari, and F. Mauri, Phys. Rev. B **75**, 035427 (2007).
[32] H. Farhat, H. Son, G. G. Samsonidze, S. Reich, M. S. Dresselhaus, and J. Kong, Phys. Rev. Lett. **99**, 145506 (2007).
[33] T. Ando, T. Nakanishi, and R. Saito, J. Phys. Soc. Jpn. **67**, 2857 (1998).
[34] C. T. White and J. W. Mintmire, Nature (London) **394**, 29 (1998).
[35] W. Liang, M. Bockrath, D. Bozovic, J. H. Hafner, M. Tinkham, and H. Park, Nature (London) **411**, 665 (2001).
[36] Z. Yao, C. L. Kane, and C. Dekker, Phys. Rev. Lett. **84**, 2941 (2000).
[37] A. Javey, J. Guo, M. Paulsson, Q. Wang, D. Mann, M. Lundstrom, and H. Dai, Phys. Rev. Lett. **92**, 106804 (2004).
[38] J.-Y. Park, S. Rosenblatt, Y. Yaish, V. Sazonova, H. Ustunel, S. Braig, T. Arias, P. Brouwer, and P. McEuen, Nano Lett. **4**, 517 (2004).
[39] M. A. Kuroda, A. Cangellaris, and J.-P. Leburton, Phys. Rev. Lett. **95**, 266803 (2005).
[40] E. Pop, D. Mann, J. Cao, Q. Wang, K. Goodson, and H. Dai, Phys. Rev. Lett. **95**, 155505 (2005).
[41] V. Perebeinos, J. Tersoff, and Ph. Avouris, Phys. Rev. Lett. **94**, 086802 (2005).
[42] S. Roche, J. Jiang, L. E. F. Foa Torres, and R. Saito, J. Phys.: Condens. Matter **19**, 183203 (2007).
[43] M. Lazzeri, S. Piscanec, F. Mauri, A. C. Ferrari, and J. Robertson, Phys. Rev. Lett. **95**, 236802 (2005).
[44] M. Lazzeri and F. Mauri, Phys. Rev. B **73**, 165419 (2006).
[45] C. Auer, F. Schurrer, and C. Ertler, Phys. Rev. B **74**, 165409 (2006).
[46] M. Oron-Carl and R. Krupke, Phys. Rev. Lett. **100**, 127401 (2008).
[47] M. Gheorghe, R. Gutierrez, N. Ranjan, A. Pecchia, A. D. Carlo, and G. Cuniberti, Europhys. Lett. **71**, 438 (2005).
[48] S. Roche, J. Jiang, F. Triozon, and R. Saito, Phys. Rev. Lett. **95**, 076803 (2005).
[49] H. Ishii, N. Kobayashi, and K. Hirose, Phys. Rev. B **76**, 205432 (2007).
[50] J. Kröger, Rep. Prog. Phys. **69**, 899 (2006).
[51] G. G. Samsonidze, E. B. Barros, R. Saito, J. Jiang, G. Dresselhaus, and M. S. Dresselhaus, Phys. Rev. B **75**, 155420 (2007).
[52] L. E. F. Foa Torres and S. Roche, Phys. Rev. Lett. **97**, 076804 (2006); Appl. Phys. A: Mater. Sci. Process. **86**, 283 (2007).
[53] L. E. F. Foa Torres and S. Roche, Phys. Rev. B **75**, 153402

(2007).
[54] W. P. Su, J. R. Schrieffer, and A. J. Heeger, Phys. Rev. Lett. **42**, 1698 (1979).
[55] D. Porezag, T. Frauenheim, T. Kohler, G. Seifert, and R. Kaschner, Phys. Rev. B **51**, 12947 (1995).
[56] Note that here we take real instead of complex polarizations for the *K* point phonons, which in turn gives real matrix elements. This can be considered as a crude model that retains the main ingredient which is the symmetry of the phonon mode.
[57] D. C. Mattis and W. D. Langer, Phys. Rev. Lett. **25**, 376 (1970).
[58] E. V. Anda, S. Makler, H. M. Pastawski, and R. G. Barrera, Braz. J. Phys. **24**, 330 (1994).
[59] J. Bonča and S. A. Trugman, Phys. Rev. Lett. **75**, 2566 (1995); H. Ness and A. J. Fisher, *ibid.* **83**, 452 (1999).
[60] E. G. Emberly and G. Kirczenow, Phys. Rev. B **61**, 5740 (2000).
[61] N. Mingo, L. Yang, J. Han, and M. Anantram, Phys. Status Solidi B **226**, 79 (2001).